Hyperfine Interact (2014) 228:141–150
DOI 10.1007/s10751-014-1019-6

The Gbar project, or how does antimatter fall?

Paul Indelicato · G. Chardin · P. Grandemange · D. Lunney · V. Manea · A. Badertscher · P. Crivelli · A. Curioni · A. Marchionni · B. Rossi · A. Rubbia · V. Nesvizhevsky · D. Brook-Roberge · P. Comini · P. Debu · P. Dupré · L. Liszkay · B. Mansoulié · P. Pérez · J.-M. Rey · B. Reymond · N. Ruiz · Y. Sacquin · B. Vallage · F. Biraben · P. Cladé · A. Douillet · G. Dufour · S. Guellati · L. Hilico · A. Lambrecht · R. Guérout · J.-P. Karr · F. Nez · S. Reynaud · C. I. Szabo · V.-Q. Tran · J. Trapateau · A. Mohri · Y. Yamazaki · M. Charlton · S. Eriksson · N. Madsen · D.P. van der Werf · N. Kuroda · H. Torii · Y. Nagashima · F. Schmidt-Kaler · J. Walz · S. Wolf · P.-A. Hervieux · G. Manfredi · A. Voronin · P. Froelich · S. Wronka · M. Staszczak

Published online: 4 February 2014

Abstract The Einstein classical Weak Equivalence Principle states that the trajectory of a particle is independent of its composition and internal structure when it is only submitted to gravitational forces. This fundamental principle has never been directly tested with antimatter. However, theoretical models such as supergravity may contain components inducing repulsive gravity, thus violating this principle. The GBAR project (Gravitational Behaviour of Antihydrogen at Rest) proposes to measure the free fall acceleration of ultracold neutral antihydrogen atoms in the terrestrial gravitational field. The experiment consists in preparing antihydrogen ions (one antiproton and two positrons) and sympathetically cool them with Be^+ ions to a few $10\,\mu$K. The ultracold ions will then be photoionized just above threshold, and the free-fall time over a known distance measured. In this work, the GBAR project is described as well as possible improvements that use quantum reflection of antihydrogen on surfaces to use quantum methods of measurements.

Proceedings of the 11th International Conference on Low Energy Antiproton Physics (LEAP 2013) held in Uppsala, Sweden, 10–15 June, 2013

G. Chardin · P. Grandemange · D. Lunney · V. Manea
CSNSM, CNRS, IN2P3, Université Paris Sud - Paris XI, Orsay, France

A. Badertscher · P. Crivelli · A. Curioni · A. Marchionni · B. Rossi · A. Rubbia
IPP, ETHZ, 8093 Zürich, Switzerland

V. Nesvizhevsky
Institut Laue-Langevin (ILL), 6 rue Jules Horowitz, 38042 Grenoble, France

D. Brook-Roberge · P. Comini · P. Debu · P. Dupré · L. Liszkay · B. Mansoulié · P. Pérez · J.-M. Rey · B. Reymond · N. Ruiz · Y. Sacquin · B. Vallage
IRFU, CEA, Saclay, 91191 Gif-sur-Yvette Cedex, France

Keywords Antihydrogen · Gravitation · Free fall · Sympathetic cooling · Weak equivalence principle

1 Introduction

Since the original paper of J. Sherck [1], there has been many works dealing with the possibility or impossibility of antigravity, i.e., on the possibility that the gravitational interaction between matter and antimatter could be repulsive or at least significantly different from the interaction with matter [2–8]. Although several tests have been performed (see, e.g., [9–11]), none concerned the direct measurement of the free fall of antimatter. It was also argued that tests on ordinary matter could yield the same information as with antimatter[12], at least for some specific theories. Yet this is not generally accepted [13].

Attempts have been made directly on antiprotons [14], but did not succeed due to the fact that gravitation is so weak compared to electrostatic interaction. There are now two accepted project at CERN, AEGIS [15] and GBAR [16], that propose methods to measure

F. Biraben · P. Cladé · A. Douillet · G. Dufour · S. Guellati · L. Hilico · P. Indelicato (✉) · A. Lambrecht · R. Guérout · J.-P. Karr · F. Nez · S. Reynaud · C. I. Szabo · V.-Q. Tran · J. Trapateau
Laboratoire Kastler Brossel, École Normale Supérieure, CNRS, Université P. et M. Curie – Paris 6, Case 74; 4, place Jussieu, 75252 Paris CEDEX 05, France
e-mail: Paul.Indelicato@spectro.jussieu.fr

A. Douillet · L. Hilico · J.-P. Karr
Université d'Evry Val d'Essonne, Évry 91025, France

A. Mohri · Y. Yamazaki
Atomic Physics Laboratory, RIKEN, 2-1 Hirosawa, Wako, Saitama 351-0198, Japan

M. Charlton · S. Eriksson · N. Madsen · D.P. van der Werf
Department of Physics, Swansea University, Swansea SA2 8PP, UK

N. Kuroda · H. Torii
Institute of Physics, University of Tokyo, 3-8-1 Komaba, Meguro, Tokyo 153-8902, Japan

Y. Nagashima
Department of Physics, Tokyo University of Science, 1-3 Kagurazaka, Shinjuku, Tokyo 162-8601, Japan

J. Walz · F. Schmidt-Kaler · S. Wolf
Johannes Gutenberg-Universität Mainz, Institut für Physik, QUANTUM, Staudingerweg 7, 55128 Mainz, Germany

P.-A. Hervieux · G. Manfredi
Université de Strasbourg (UDS), Institut de Physique et Chimie des Matériaux de Strasbourg (IPCMS), Département d'Optique ultrarapide et de Nanophotonique (DON), 23, rue du Loess - BP 43 - 67034 Strasbourg Cedex, France

A. Voronin · P. Froelich
P. N. Lebedev Physical Institute, 53 Leninsky Prospect, 117924 Moscow, Russia

S. Wronka · M. Staszczak
National Centre for Nuclear Research, 05-400 Otwock, Ŝwierk, Poland

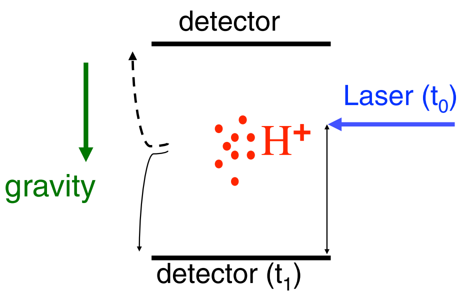

Fig. 1 Principle of the gbar experiment. The $\bar{H}^+$ ions are cooled to 10 μk

directly the free-fall of cold or ultracold antihydrogen. Recently, the ALPHA experiment reported a preliminary result using trapped antihydrogen, with wide error bars [17].

The GBAR project, described in this paper, is based on the proposition of [18]. It recognizes that direct laser cooling of hydrogen does not allow to cool down to low enough temperature. The principle of the experiment as presented in Ref. [18] is to produce $\bar{H}^+$ ions and cool them by sympathetic cooling of an other ion like Be^+. The $\bar{H}^+$ ions are obtained by the interaction of slow antiprotons with a cloud of positronium atoms. Sympathetic cooling, using, e.g., Be^+ ions allows reaching a temperature of the order of 10 μK, that corresponds to a velocity of less than 1 m/s. The resulting $\bar{H}^+$ ion is then photodetached using a laser just above threshold with a laser direction and polarization such that the $\bar{H}$ will be produced with minimum vertical impulsion. This process is represented in Fig. 1. The $\bar{H}$ atoms will then fall with a very small initial vertical velocity and be detected some 30 cm below. This allows for a measurement with an accuracy of 0.001 if 5×10^5 $\bar{H}$ atoms can be detected.

2 Description of the experiment

The complete synoptic scheme of the experiment is presented on Fig. 2. The experimental setup is composed of 3 main parts. The lower part of Fig. 2 concerns the antiprotons. The antiproton extracted from the CERN AD with an energy of 5.3 MeV will be slowed down and cooled using the future electrostatic ring ELENA [19] to 100 keV for better deceleration efficiency. Further slowing down will be done using a pulsed drift tube as done in ISOLDE at CERN with heavy ions [20, 21]. The antiprotons must be finally decelerated to 1 keV and focussed into the 1 mm diameter tube that will contain the positronium (Ps) target.

Obtaining a dense enough positronium target, with a density of $\approx 10^{12}$ cm^{-3} requires an intense beam of positrons. The central part of Fig. 2 shows the scheme we have selected. A 10 MeV, 0.2 mA LINAC will be used to produce a fast positron beam (MeV). These positron are decelerated by interaction with a set of tungsten meshes used as moderator, with an aimed efficiency of 5×10^{-4}. The positrons are then accumulated in a Penning trap containing 2×10^{10} trapped electrons for cooling. The electrons are trapped in a 1 keV deep well, while the positrons are trapped in a variable depth well, which will vary from 50 eV at the beginning to $\approx$ 1 keV at the end of the accumulation time. We use a Penning–Malmberg trap developped in RIKEN[22], that has been able to cool and store 10^6 positrons. The accumulation can be done in 110 s, the period between two antiproton bursts. In order to reach the required density of positronium, the system must be able to produce $\approx 10^{10}$ Ps in 0.01 cm^3 tube. The positroniums are created with a 30 % efficiency by the conversion of positrons interacting with a porous sicilica coating inside a hollow tube. We thus need to produce 3×10^{10} positrons.

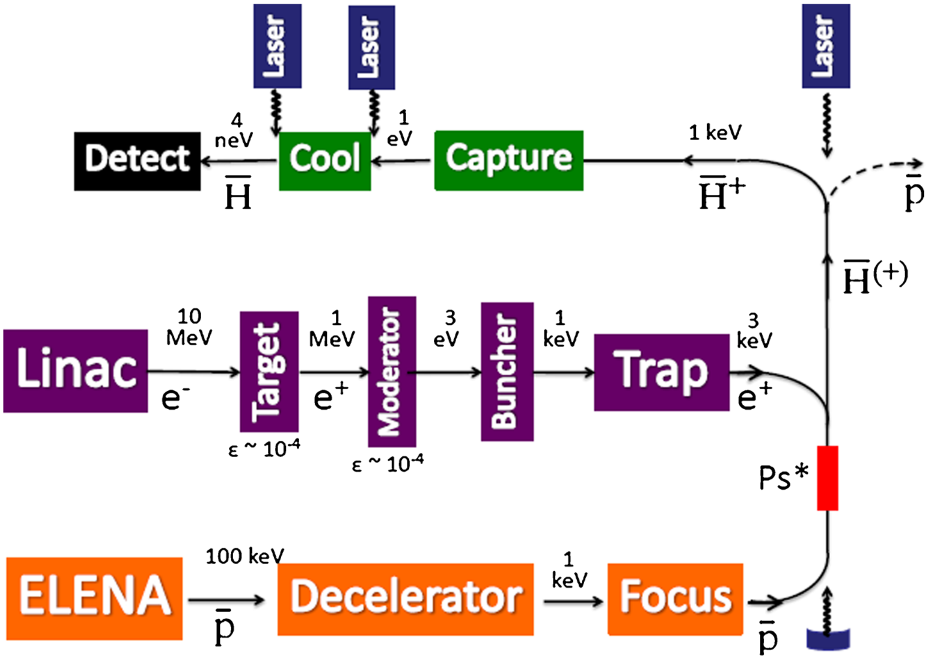

Fig. 2 Schematics of the gbar project

The efficiency of ortho-positronium (the long-lived, 142 ms, state) production by different samples of porous silica has been measured [23] as well as its cooling [24, 25]. The instantaneous flux in the test experiments was close to what is required in GBAR.

It is possible to excite the positronium in order to increase the efficiency of $\bar{\mathrm{H}}^+$ production. The $\bar{\mathrm{H}}^+$ production is a two-step process. First an $\bar{\mathrm{H}}$ atom is produced, then it captures a positron from a second Ps. The efficiency for producing $\bar{\mathrm{H}}$ goes as n^4, where n is the Ps principal quantum number. The binding energy of the $\bar{\mathrm{H}}^+$ ion is the same as the one of the H^- one, 0.76 eV, which is very close to the excitation energy of Ps in the $n = 3$ level, thus leading to a possible resonant excitation process. A detailed description of the processes and estimation of the needed cross sections can be found in [26].

3 Capture and cooling of the $\bar{\mathrm{H}}^+$ ions

The $\bar{\mathrm{H}}^+$ ions are produced at an energy of around 1 keV with an energy spread of $\approx$ 20 eV. They need to be decelerated and cooled to 10 μK, i.e., by 12 orders of magnitude. The process is described in the upper part of Fig. 2. The 1 keV $\bar{\mathrm{H}}^+$ must be decelerated to an energy of a few eV and captured in a Paul trap. The capture trap must be able to accommodate ions with an energy spread of 20 eV. A cloud of Doppler-cooled Be^+ is used to sympathetically cool the captured $\bar{\mathrm{H}}^+$ ions to the mK range. This require that the trap can accommodate simultaneously the $\bar{\mathrm{H}}^+$ ions and the Be^+, which have a mass ratio of 9.

Several tunable laser schemes to photoionize Be atoms and cool efficiently the Be^+ ions have been proposed recently, using all solid-state design, using either laser diode [27, 28] or fiber lasers [29, 30]. At the present time, the NIST solution for a 313 nm laser, which

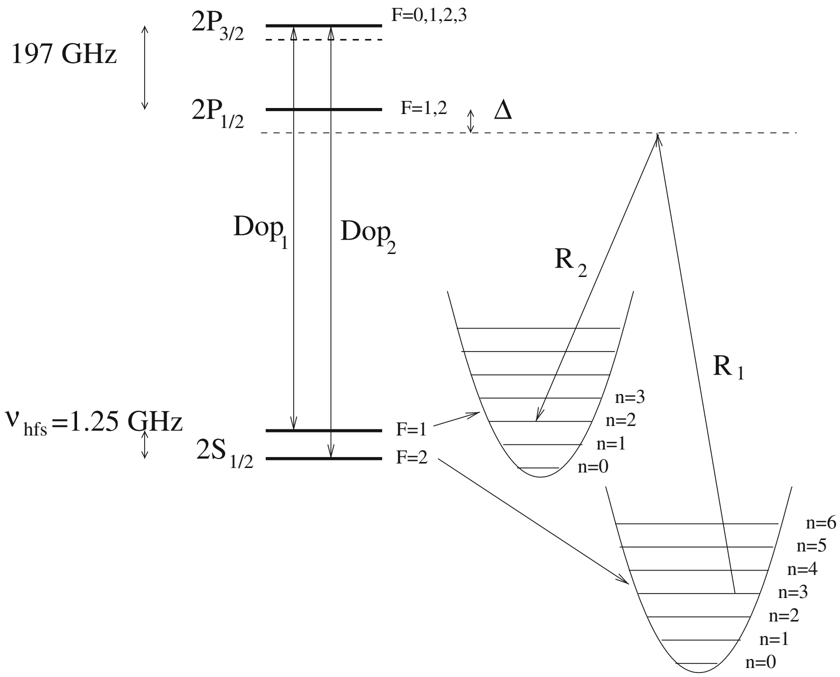

Fig. 3 Be^{+} ion level scheme (*left*) and principle of the two-ions Raman cooling (*right*). Dop_2 and Dop_1 transitions are used for cooling, detection and repumping. The harmonic oscillator energy of the center of mass motion in one of the eigenmode of the ion pair is represented. R_1 and R_2 are the Raman excitation beams

provide up to 750 mW of power, seems to be the most practical one. The Be^{+} transition wavelength is around 313.13 nm, in the UV. The level scheme of Be^{+} is presented in Fig. 3. The Dop_2 line at 313.13 nm is used for cooling and detection. Line Dop_1 is used for repumping from the $F = 1$ hyperfine level.

Sympathetic cooling is a well established technique [31] that can ultimately be applied for quantum logic experiment [32]. The $\bar{H}^{+}$ ions will stay at the center of the trap, surrounded by the Be^{+} ions. Once the $\bar{H}^{+}$ ions have been cooled to mK temperatures, the next step transfer the $\bar{H}^{+}$ ions into the precision trap and to use Raman sideband cooling [33] to obtain the required μK temperature. The principle of Raman sideband cooling is presented in Fig. 3.

The Raman sideband cooling works by coherently driving stimulated Raman transitions between the state $|F = 2, n\rangle$ to $|F = 1, n - 1\rangle$ and spontaneous Raman transitions from $|F = 1, n - 1\rangle$ to $|F = 2, n - 1\rangle$ using so called Raman pulses. As a result, the vibrational number is decreased by one unit. By repeating this procedure, one can prepare the ion in the fundamental vibration level. The stimulated Raman transition is driven by the counter-propagating beams R_1 and R_2 with Raman lasers far detuned from the 2S→2P transition to avoid spontaneous emission, with frequencies satisfying the resonance condition $\omega_{R_1} - \omega_{R_2} = \omega_{\text{hfs}} + \omega_{\text{vibr}}$. ω_{vibr} corresponds to the frequency in the harmonic potential in Fig. 3 and ω_{hfs} is the lower level hyperfine frequency splitting. The spontaneous Raman transition is driven close to the Dop_1 beam at 313.198 nm. In the Lamb-Dicke regime where $\hbar\omega_{\text{vibr}} \gg E_{\text{recoil}}$, the spontaneous emission mainly occurs with $\Delta n = 0$.

In order to resolve the macromotion sidebands in the trap, the trapping potential has to be very steep, so that the frequencies of the motion in the 3 directions of space are in the MHz range. The Raman sideband cooling of Be^+ proceeds from the level n in the potential well created by the Paul trap, and an ion in the $^2S_{1/2},\ F = 2$ level. The cooling sequence is then $(F = 1, n-1)$, $(F = 2, n-1)$, $(F = 1, n-2)$, $(F = 2, n-2)\ldots$, $(F = 2, 0)$. It has been shown that the ions spend ≈98 % of the time in the $n = 0$ level in 1D and 92 % in 3D [34].

The number of eigen-frequencies ω_{vibr} to generate varies like $3 \times N$, where N is the number of ions. The system is practical if only a few ions are trapped. We plan to have only two, one Be^+ and one $\bar{H}^+$ in the precision trap.

A difficult issue to apply sympathetic cooling in the case of $\bar{H}^+$ is that the cooling lasers provide energies way above the ionization threshold of $\bar{H}^+$ (3.97 eV vs 0.76 eV). Special care will have to be taken not to photoionize the $\bar{H}^+$ ion during the Doppler and Raman cooling phase. This process limits the cooling time to ≤ 500 ms. If longer times are needed, one can use of doughnut-shaped laser beams and tight focussing of the laser on the Be^+ ion during the Raman cooling of the ion pair.

Another issue is the number of Be^+ ions needed to cool the high energy $\bar{H}^+$ ions in the initial phase. Simulations show that a very large number is required, depending on the cloud aspect ratio diameter/length. Typically for aspect ratios of the Be^+ ion clouds ranging from 1/5 to 1/8, one needs 10^6 to 10^7 ions. The cooling time will have to be investigated with simulations and tested on H_2^+ or protons. Some simulations hint that the process should last around 1 s [35]. Yet, if the process is not fast enough, and the cooling times becomes comparable to the time between antiproton pulses from ELENA, an additional step, using resistive cooling to 4 K could be needed.

4 Photodetachment and detection

The photodetachment must be done in conditions that do not yield too large a vertical speed. The photon energy must be just above threshold. The absorption of a 0.76 eV photon gives to the resulting $\bar{H}$ atom a recoil velocity of 0.2 m/s. The laser beam must then be horizontal. The displacement of the atom due to this horizontal initial speed is 4 cm for a free fall of 0.2 s. The recoil due to the emission of the positron is 0.3 m/s for a laser energy 1 μeV above threshold. Both speeds are of the same order of magnitude as the thermal speed distribution of the cold ions. Yet, the detachment cross-section strongly decreases close to the threshold. One must find an optimum between minimizing the $\bar{H}$ recoil velocity and having a large enough photodetachment rate.

The 1.64 μm laser radiation for photodetachment will be produced by an optical parametric oscillator (OPO) pumped by a fiber laser at 1064 nm A non-linear crystal in the OPO (a MgO:PPLN – Periodically-Poled Lithium Niobate) converts one photon at 1.064 μm in two photons at the wavelengths of 1.64 μm (called the signal) and 3.03 μm (the idler). Such laser sources are commercially available. The non-linear crystal is placed in a ring cavity, resonant with the signal. The signal frequency is controlled with the help of an etalon placed inside the cavity and of a piezoelectric translator to scan the cavity length. For a pump power of 15 W the CW output power is 2 W for the signal and the idler. The control of the intensity of the signal radiation will be made with an acousto-optic modulator.

The photodetachment laser pulse will be the start of the free fall. A movable plate, located around 10 cm below the photodetachment area will receive the antihydrogen atoms, which will annihilate in it. The measurement chamber will be surounded by time projection Chambers (TPC's) to eliminate cosmic background and provide the trajectory information

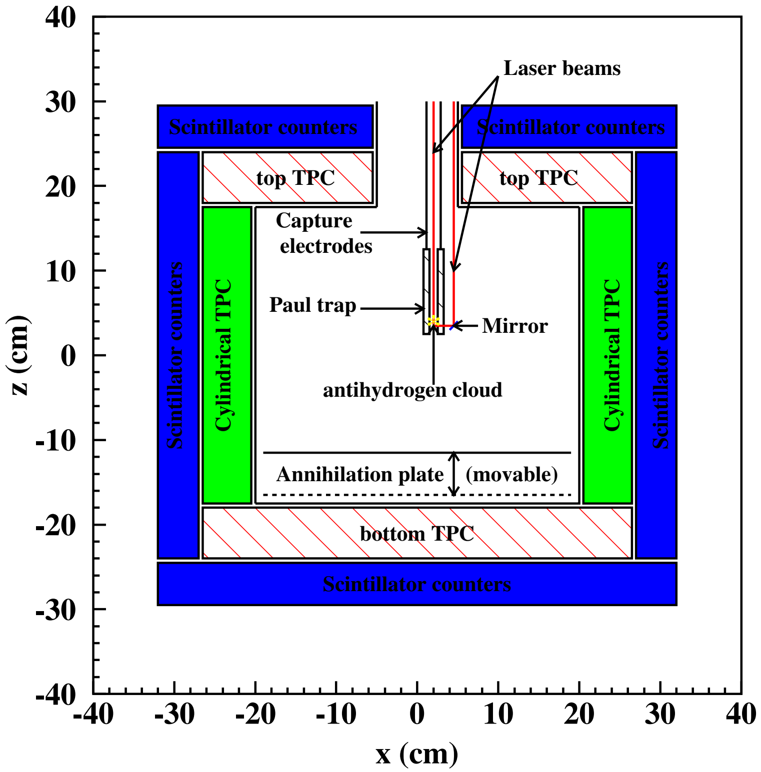

Fig. 4 Measurement chamber with the different components of the detection system

on the charged particles. Plastic scintillator counters located around the TPC's will be used to detect the charged pions from annihilation and provide the annihilation time with high precision. The detection setup is shown in Fig. 4.

The design of the precision trap where the Raman side-band cooling of the $\bar{\mathrm{H}}^+$–Be^+ pair and the photodetachment will be performed requires special attention. The trap must allow several laser access, and block as little as possible the path of the resulting $\bar{\mathrm{H}}$ atoms. We will design trap on a chip, that will be used for transport of the needed $\bar{\mathrm{H}}^+$ and Be^+ ions, for their cooling and also for separating the two species once the $\bar{\mathrm{H}}^+$ ion is cold. Such technique are being developed for possible applications in quantum information processing with ions (see, e.g., [36–38])

There is one possible problem with this detection scheme when very cold $\bar{\mathrm{H}}$ atoms are used: quantum reflection due to the Casimir potential can happen in the detector plate. This effect has been observed with ultra-cold atoms [39]. Recent calculations show that it would prevent direct contact between antihydrogen and the detector plate, thus preventing annihilation and lead to sizable reflections in the GBAR setup [40]. But this effect can be turned as an advantage, and be used to increase accuracy. Quantum states in the gravitational field have been observed with ultra-cold neutrons[41]. A few years later, the whispering gallery effect for neutron has been demonstrated [42]. This effect is now proposed for improving the accuracy of measurement of the effect of gravitation on antimatter when using ultra cold $\bar{\mathrm{H}}$ atoms as in the case of GBAR [43, 44]. This method could provide very precise measurements of the antimatter-surface interaction as well as an accurate test of the weak equivalence principle.

5 Conclusions and perspectives

We have described the GBAR experiment, which aims at measuring the free fall of ultra-cold antihydrogen atoms. The originality of the experiment is to start from sympathetically cooled $\bar{\mathrm{H}}^+$ ions to provide good accuracy. The first stage of the GBAR experiment aim at an accuracy of 1 % for the precision of the measurement of the free fall of $\bar{\mathrm{H}}$. This accuracy can be obtained using roughly 1500 events and a few weeks of beam time. An accuracy of 0.1 % can be reached with 5×10^5 event. We plan to use advanced ion cooling and manipulation techniques that have been developed for applications in ion quantum computing to have an excellent control of the $\bar{\mathrm{H}}^+$ ion produced. Finally We discussed a specific originality of GBAR, which is that a possible perturbing effect, quantum reflection on the annihilation plate of the very cold $\bar{\mathrm{H}}$ atoms, described in Section 4 can be used to increase accuracy.

Acknowledgments P.I. and C.I. Szabo have been partially supported by the Helmholtz Alliance *HA216/EMMI*. Partial financing of the project has been provided by the *Région Île de France*, DIM-IFRAF, project RESIMA (2011).

References

1. Scherk, J.: Phys. Lett. B **88**, 265 (1979). http://www.sciencedirect.com/science/article/B6TVN-46YKS47-2RB/2/014fc5 233267c60b9065828f66c4ccce
2. Nieto, M.M., Goldman, T.: Phys. Rep. **205**, 221 (1991). http://www.sciencedirect.com/science/article/B6TVP-46TY5BT-22/2/8354635bd464ffaea9ab3d82b6dd7820
3. Karshenboim, S.G.: Astron. Lett. **35**, 663 (2009). doi:10.1134/S1063773709100028
4. Kostelecký, V.A., Tasson, J.D.: Phys. Rev. D **83**, 016013 (2011). http://link.aps.org/doi/10.1103/PhysRevD.83.016013
5. Villata, M.: EPL (Europhys. Lett.) **94**, 20001 (2011). http://stacks.iop.org/0295-5075/94/i=2/a=20001
6. Benoit-Lévy, A., Chardin, G.: Astron. Astrophys. **537**(1), A78 (2012). doi:10.1051/0004-6361/201016103
7. Cabbolet, M.T.F.: Astrophys. Space Sci. **337**, 5 (2012). doi:10.1007/s10509-011-0939-8
8. Villata, M.: Astrophys. Space Sci. **337**, 15 (2012). doi:10.1007/s10509-011-0940-2
9. Hughes, R.J., Holzscheiter, M.H.: Phys. Rev. Lett. **66**, 854 (1991). http://link.aps.org/doi/10.1103/PhysRevLett.66.854
10. Gabrielse, G., Khabbaz, A., Hall, D.S., Heimann, C., Kalinowsky, H., Jhe, W.: Phys. Rev. Lett. **82**, 3198 (1999). http://link.aps.org/doi/10.1103/PhysRevLett.82.3198
11. Apostolakis, A., Aslanides, E., Backenstoss, G., Bargassa, P., Behnke, O., Benelli, A., Bertin, V., Blanc, F., Bloch, P., Carlson, P., Carroll, M., Cawley, E., Chardin, G., Chertok, M.B., Danielsson, M., Dejardin, M., Derre, J., Ealet, A., Eleftheriadis, C., Faravel, W., Fetscher, L., Fidecaro, M., Filipčič, A., Francis, D., Fry, J., Gabathuler, E., Gamet, R., Gerber, H.J., Go, A., Haselden, A., Hayman, P.J., Henry-Couannier, F., Hollander, R.W., Jon-And, K., Kettle, P.R., Kokkas, P., Kreuger, R., Le Gac, R., Leimgruber, F., Mandić, I., Manthos, N., Marel, G., Mikuž, M., Miller, J., Montanet, F., Muller, A., Nakada, T., Pagels, B., Papadopoulos, I., Pavlopoulos, P., Polivka, G., Rickenbach, R., Roberts, B.L., Ruf, T., Sakeliou, L., Schäfer, M., Schaller, L.A., Schietinger, T., Schopper, A., Tauscher, L., Thibault, C., Touchard, F., Touramanis, C., Van Eijk, C.W.E., Vlachos, S., Weber, P., Wigger, O., Wolter, M., Zavrtanik, D., Zimmerman, D., Ellis, J., Mavromatos, N.E., Nanopoulos, D.V.: Phys. Lett. B **452**, 425 (1999). http://www.sciencedirect.com/science/article/pii/S0370269399002713
12. Adelberger, E.G., Heckel, B.R., Stubbs, C.W., Su, Y.: Phys. Rev. Lett. **66**, 850 (1991). http://prl.aps.org/abstract/PRL/v66/i7/p850_1
13. Goldman, T., Nieto, M.M., Holzscheiter, M.H., Darling, T.W., Schauer, M., Schecker, J.: Phys. Rev. Lett. **67**, 1048 (1991). http://link.aps.org/doi/10.1103/PhysRevLett.67.1048

14. Holzscheiter, M.H., Brown, R.E., Camp, J.B., Cornford, S., Darling, T., Dyer, P., Goldman, T., Høibråten, S., Hosea, K., Hughes, R.J., Jarmie, N., Kenefick, R.A., King, N.S.P., Lizon, D.C., Nieto, M.M., Midzor, M.M., Parry, S.P., Rochet, J., Ristinen, R.A., Schauer, M.M., Schecker, J.A., Witteborn, F.C.: Nucl. Phys. A **558**, 709 (1993). http://www.sciencedirect.com/science/article/pii/037594749390432W
15. Drobychev, G.Y., Nédélec, P., Sillou, D., Gribakin, G., Walters, H., Ferrari, G., Prevedelli, M., Tino, G.M., Doser, M., Canali, C., Carraro, C., Lagomarsino, V., Manuzio, G., Testera, G., Zavatarelli, S., Amoretti, M., Kellerbauer, A.G., Meier, J., Warring, U., Oberthaler, M.K., Boscolo, I., Castelli, F., Cialdi, S., Formaro, L., Gervasini, A., Giammarchi, G., Vairo, A., Consolati, G., Dupasquier, A., Quasso, F., Stroke, H.H., Belov, A.S., Gninenko, S.N., Matveev, V.A., Byakov, V.M., Stepanov, S.V., Zvezhinskij, D.S., De Combarieu, M., Forget, P., Pari, P., Cabaret, L., Comparat, D., Bonomi, G., Rotondi, A., Djourelov, N., Jacquey, M., Büchner, M., Trénec, G., Vigué, J., Brusa, R.S., Mariazzi, S., Hogan, S., Merkt, F., Badertscher, A., Crivelli, P., Gendotti, U., Rubbia, A.: Proposal for the AEGIS experiment at the CERN antiproton decelerator (Antimatter Experiment: Gravity, Interferometry, Spectroscopy), Tech. Rep. SPSC-P-334. CERN-SPSC-2007-017. CERN, Geneva (2007). http://cds.cern.ch/record/1037532?ln=fr
16. Chardin, G., Grandemange, P., Lunney, D., Manea, V., Badertscher, A., Crivelli, P., Curioni, A., Marchionni, A., Rossi, B., Rubbia, A., Nesvizhevsky, V., Hervieux, P.-A., Manfredi, G., Comini, P., Debu, P., Dupré, P., Liszkay, L., Mansoulié, B., Pérez, P., Rey, J.-M., Ruiz, N., Sacquin, Y., Voronin, A., Biraben, F., Cladé, P., Douillet, A., Gérardin, A., Guellati, S., Hilico, L., Indelicato, P., Lambrecht, A., Guérout, R., Karr, J.-P., Nez, F., Reynaud, S., Tran, V.-Q., Mohri, A., Yamazaki, Y., Charlton, M., Eriksson, S., Madsen, N., van der Werf, D.-P., Kuroda, N., Torii, H., Nagashima, Y.: Proposal to measure the Gravitational Behaviour of Antihydrogen at Rest, Tech. Rep. CERN-SPSC-2011-029. SPSC-P-342. CERN, Geneva (2011). http://cds.cern.ch/record/1386684?ln=en
17. Alpha Collaboration, Charman, A.E.: Nat. Commun. **4**, 1785 (2013). doi:10.1038/ncomms2787
18. Walz, J., Hänsch, T.W.: Gen. Relativ. Gravit. **36**, 561 (2004). doi:10.1023/B:GERG.0000.010730.93408.87
19. Tranquille, G., Belochitskii, P., Eriksson, T., Maury, S., Oelert, W.: Conf. Proc. **C1205201**, THPPP017. 3 (2012)
20. Herfurth, F., Dilling, J., Kellerbauer, A., Bollen, G., Henry, S., Kluge, H.J., Lamour, E., Lunney, D., Moore, R.B., Scheidenberger, C., Schwarz, S., Sikler, G., Szerypo, J.: Nucl. Instr. Methods A **469**, 254 (2001). http://www.sciencedirect.com/science/article/B6TJM-43PGJKX-D/2/d5a71a85b9a62763e751fb5a1fcb3716
21. Lunney, D., Bachelet, C., Guénaut, C., Henry, S., Sewtz, M.: Nucl. Instr. Methods A **598**, 379 (2009). http://www.sciencedirect.com/science/article/pii/S0168900208014459
22. Oshima, N., Kojima, T.M., Niigaki, M., Mohri, A., Komaki, K., Yamazaki, Y.: Phys. Rev. Lett. **93**, 195001 (2004). http://link.aps.org/doi/10.1103/PhysRevLett.93.195001
23. Liszkay, L., Corbel, C., Perez, P., Desgardin, P., Barthe, M.-F., Ohdaira, T., Suzuki, R., Crivelli, P., Gendotti, U., Rubbia, A., Etienne, M., Walcarius, A.: Appl. Phys. Lett. **92**, 063114 (2008). doi:10.1063/1.2844888. http://link.aip.org/link/?APL/92/063114/1
24. Cassidy, D.B., Crivelli, P., Hisakado, T.H., Liszkay, L., Meligne, V.E., Perez, P., Tom, H.W.K., Mills, A.P.: Phys. Rev. A **81**, 012715 (2010). http://link.aps.org/doi/10.1103/PhysRevA.81.012715
25. Crivelli, P., Gendotti, U., Rubbia, A., Liszkay, L., Perez, P., Corbel, C.: Phys. Rev. A **81**, 052703 (2010). http://link.aps.org/doi/10.1103/PhysRevA.81.052703
26. Comini, P., Hervieux, P.-A., Biraben, F.: These proceedings, Hyperfine Interaction. doi:10.1007/s10751-014-1030-y
27. Ball, H., Lee, M.W., Gensemer, S.D., Biercuk, M.J.: Rev. Sci. Instrum. **84**, 063107 (2013). doi:10.1063/1.4811093
28. Lo, H.-Y., Alonso, J., Kienzler, D., Keitch, B.C., Clercq, L.E., Negnevitsky, V., Home, J.P.: Appl. Phys. B, 1 (2013). doi:10.1007/s00340-013-5605-0
29. Vasilyev, S., Nevsky, A., Ernsting, I., Hansen, M., Shen, J., Schiller, S.: Appl. Phys. B Lasers Opt. **103**, 27 (2011). doi:10.1007/s00340-011-4435-1
30. Wilson, A.C., Ospelkaus, C., VanDevender, A.P., Mlynek, J.A., Brown, K.R., Leibfried, D., Wineland, D.J.: Appl. Phys. B **105**, 741 (2011). doi:10.1007/s00340-011-4771-1
31. Larson, D.J., Bergquist, J.C., Bollinger, J.J., Itano, W.M., Wineland, D.J.: Phys. Rev. Lett. **57**, 70 (1986). http://link.aps.org/doi/10.1103/PhysRevLett.57.70
32. Barrett, M.D., DeMarco, B., Schaetz, T., Meyer, V., Leibfried, D., Britton, J., Chiaverini, J., Itano, W.M., Jelenkovicacute, B., Jost, J.D., Langer, C., Rosenband, T., Wineland, D.J.: Phys. Rev. A **68**, 042302 (2003). http://link.aps.org/doi/10.1103/PhysRevA.68.042302
33. Heinzen, D.J., Wineland, D.J.: Phys. Rev. A **42**, 2977 (1990). http://link.aps.org/doi/10.1103/PhysRevA.42.2977

34. Monroe, C., Meekhof, D.M., King, B.E., Jefferts, S.R., Itano, W.M., Wineland, D.J., Gould, P.: Phys. Rev. Lett. **75**, 4011 (1995). http://link.aps.org/doi/10.1103/PhysRevLett.75.4011
35. Bussmann, M., Schramm, U., Habs, D., Kolhinen, V.S., Szerypo, J.: Int. J. Mass Spectrom. **251**, 179 (2006). http://www.sciencedirect.com/science/article/B6VND-4JGJGXH-1/2/c3e1265f6ef86a3c9bfa07c0eab0d64e
36. Eble, J.F., Ulm, S., Zahariev, P., Schmidt-Kaler, F., Singer, K.: J. Opt. Soc. Am. B **27**, A99 (2010). http://josab.osa.org/abstract.cfm?URI=josab-27-6-A99
37. Huber, G., Ziesel, F., Poschinger, U., Singer, K., Schmidt-Kaler, F.: Appl. Phys. B **100**, 725 (2010). doi:10.1007/s00340-010-4148-x
38. Walther, A., Ziesel, F., Ruster, T., Dawkins, S.T., Ott, K., Hettrich, M., Singer, K., Schmidt-Kaler, F., Poschinger, U.: Phys. Rev. Lett. **109**, 080501 (2012). http://link.aps.org/doi/10.1103/PhysRevLett.109.080501
39. Shimizu, F.: Phys. Rev. Lett. **86**, 987 (2001). http://link.aps.org/doi/10.1103/PhysRevLett.86.987
40. Dufour, G., Gérardin, A., Guérout, R., Lambrecht, A., Nesvizhevsky, V.V., Reynaud, S., Voronin, A.Y.: Phys. Rev. A **87**, 012901 (2013). http://link.aps.org/doi/10.1103/PhysRevA.87.012901
41. Nesvizhevsky, V.V., Borner, H.G., Petukhov, A.K., Abele, H., Baeszler, S., Ruesz, F.J., Stoferle, T., Westphal, A., Gagarski, A.M., Petrov, G.A., Strelkov, A.V.: Nature **415**, 297 (2002). doi:10.1038/415297a
42. Nesvizhevsky, V.V., Voronin, A.Y., Cubitt, R., Protasov, K.V.: Nat. Phys. **6**, 114 (2010). doi:10.1038/nphys1478
43. Voronin, A.Y., Nesvizhevsky, V.V., Reynaud, S.: Phys. Rev. A **85**, 014902 (2012). http://link.aps.org/doi/10.1103/PhysRevA.85.014902
44. Voronin, A.Y., Nesvizhevsky, V.V., Reynaud, S.: J. Phys. B: At. Mol. Opt. Phys. **45**, 165007 (2012). http://stacks.iop.org/0953-4075/45/i=16/a=165007